Maximum entropy method for phase-unstable aperture synthesis

R.K. Shevgaonkar[1,2]

[1] Indian Institute of Astrophysics, Bangalore 560034, India
[2] Astronomy Program, University of Maryland College Park, MD 20742, USA

Summary. An application of the Maximum Entropy Method to the closure data is described here. It is shown that although the basic principle of the method is to obtain a brightness distribution which has highest entropy the closure phases play a prominent role in giving the correct reconstruction especially when the distributions are complex and the measurement errors are large. The method gives faithful reconstruction for the observed random phase error up to $\pm 150°$. The method can be used as an alternative to the routinely used 'self-calibration' technique to improve the astronomical images obtained from the phase unstable interferometers. For large fields of view when due to repetitive use of CLEAN the 'self-calibration' method becomes time consuming, MEM with closure phase may have a computational advantage. For extended sources as the performance of CLEAN deteriorates the maximum entropy method could be superior to the self-calibration.

Key words: image processing – maximum entropy – radio astronomy; closure phase – interferometry

1. Introduction

In radio astronomy one is interested in obtaining an image of the brightness distribution in the sky with as high a resolution as possible. The application of aperture synthesis technique was a major advancement in the direction of the resolution improvement. However, soon it became apparent that due to large measurement errors the quality of the synthesized maps is quite restricted. In the presence of the measurement errors the observed map is contaminated by spurious positive and negative sources. Also, in the presence of these errors the image deconvolution techniques like CLEAN or Maximum Entropy Method (MEM) are unable to provide faithful deconvolution of the image although they work outstandingly on the error-free model maps. Therefore, before going for the problem of deconvolution, it is worthwhile to explore a possibility of the refinement of the measurement errors in the observed visibilities.

In the past few years, considerable progress has been made in the direction of improving the maps obtained from unstable interferometers (Cornwell and Wilkinson, 1981; Readhead and

Wilkinson, 1978; Readhead et al., 1980). The success of these image improving techniques lies in the use of so called 'closure' phase which provides almost as much information about the visibility phases as the true visibilities themselves. The method which uses the closure phase information for refining the measured phase errors is called the 'self-calibration' technique and the reconstructed maps are known as 'hybrid maps' (Baldwin and Warner, 1976). The self-calibration method is essentially an iterative technique which is a combination of the image deconvolution method CLEAN (Högbom, 1974) and the closure phases. The method starts with a model distribution which assigns the phases to some of the observed visibility amplitudes and the remaining are computed through the closure relations. Presently, the method is used more or less routinely to improve the radio maps. However, the final restored distribution is quite sensitive to the choice of the starting model and at many occasions it has been observed that due to improper starting model the method gives a bad reconstruction. For the brightness distributions which are composed of point-like sources the guess of model distribution could be relatively easy but for extended distributions, especially when the errors are large, it is not always possible to predict the correct starting model. Further, due to the repetitive use of 'CLEAN' the method becomes quite expensive in computer time especially for large fields of view (Cornwell and Evans, 1985).

The maximum entropy method has shown a new promise in the field of astronomical image reconstruction. In radio astronomy, the method has essentially been used as an image deconvolution technique. However, in other fields like crystallography, the method has been proposed for the phase refinement problem (Narayan and Nityananda, 1981, 1982). The MEM assigns the phases to the observed amplitudes in such a way that the entropy of the distribution is maximized. In crystallography problems where the sources are well isolated point-like sources (atoms) the maximization of entropy provides reasonably good reconstruction. However, in radio astronomy where the presence of extended sources is common, only maximization of entropy does not give good image reconstruction if the measurement errors are large. Considering the cyclic nature of the phase, there could be multiple maxima of the entropy, all of which would not correspond to the true distribution. In the absence of any additional constraints the solution may be trapped in any of the wrong maxima to give bad reconstruction. To obtain the correct distribution, the solution should be guided to the proper maximum through additional constraints. These constraints could be in the form of closure phases. We discuss here an application of the MEM combined with the closure phases to the phase refinement problem in radio

350

astronomy. In the second section we briefly mention the principle of the closure phase and in the third section we present a mathematical formulation of the MEM applied to the closure data. In the fourth section, we discuss the computational implementation of the method along with some results and in the fifth section we analyse the effect of noise on the method. At the end we make some concluding remarks.

2. Closure phase

For strong sources which have a high signal-to-noise ratio, the phase errors could be mainly introduced by the changes in the path lengths due to variable atmosphere and the temperature sensitive electronics, and the positional accuracy of the interferometer elements. The concept of closure phase which is free from all these errors was first introduced by Jennison in 1958. The basic idea of the closure phase could be explained by an example of three element interferometer system. Figure 1 shows three antennas A, B and C forming three interferometer pairs AB, BC and CA. Let ζ_{AB}, ζ_{BC} with ζ_{CA} represent the true phases of the Fourier transform of the brightness distribution at spacings AB, BC and CA respectively. If ψ_A, ψ_B and ψ_C are the phase errors introduced by the position of the source in relation to the collimation plane at A, B and C, and δ_A, δ_B and δ_C are the phase errors due to atmospheric path lengths and the front end instruments at A, B and C respectively, the observed phases of the three Fourier components with baselines AB, BC and CA are

$$\phi_{AB} = \zeta_{AB} + (\psi_B - \psi_A) + (\delta_B - \delta_A)$$
$$\phi_{BC} = \zeta_{BC} + (\psi_C - \psi_B) + (\delta_C - \delta_B) \tag{1}$$
$$\phi_{CA} = \zeta_{CA} + (\psi_A - \psi_C) + (\delta_A - \delta_C)$$

where ϕ_{xy} is the observed phase at y with respect to the phase at x; $\phi_{xy} = -\phi_{yx}$.

The sum of the three observed Fourier phases

$$\phi = \phi_{AB} + \phi_{BC} + \phi_{CA} \tag{2}$$

is also equal to the sum of the three true Fourier phases. This quantity ϕ is independent of all the systematic errors and is called the 'closure' phase. It is clear that the closure phase is free from
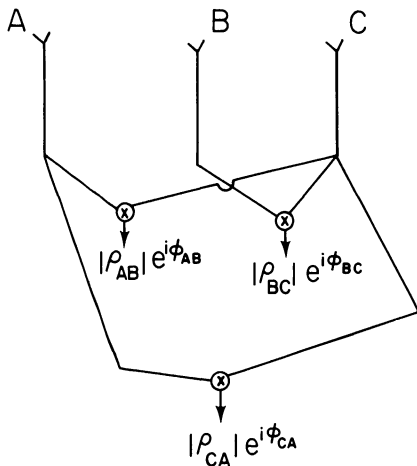
the systematic measurement errors irrespective of the separation and orientation of the interferometer baselines. Moreover, Eq. (2) is not true for only three element system but can be obtained for any system consisting of three or more interferometer elements. Essentially, the statement of closure phase is 'the sum of all visibility phases around a close loop of interferometers is free from all the systematic measurement errors'. For a system of N elements i.e., $N(N - 1)/2$ visibilities, the total number of loops and therefore the total number of closure phases is

$$N_C = {}^NC_3 + {}^NC_4 + \cdots + {}^NC_N \tag{3}$$

However, it should be noted that all the N_C closure equations are not independent. For an N-element interferometer system there could be maximum N errors associated with the $N(N - 1)/2$ visibilities. Further, since the visibility phase is only a difference between the phases of signals from two elements of an interferometer, any one of the antennas can be assigned an arbitrary phase and all other phases could be referred to that. Hence, in an N element system there are $(N - 1)$ rather than N unknown phase errors giving total independent closure phases $p = N(N - 1)/2 - (N - 1) = (N - 1)(N - 2)/2$.

For a system of N interferometer elements there will be p closure relations of type (2) which in general can be represented by a matrix notation of kind

$$A \cdot \phi = \phi_C \tag{4}$$

Where, A is a $p \times q$ rectangular matrix ($p < q$) having elements 0 or ± 1; ϕ is a vector of q unknown phases and ϕ_C is a vector of p closure phases. The number of visibility phases is always greater than the total closure equations and therefore there are infinite distributions which satisfy the closure phases. To obtain a unique solution we need to have more information about the distribution along with the closure phases. In self-calibration the additional information about the source is provided in the form of a model distribution. In the maximum entropy method, among the infinite solutions given by closure relations we propose to accept that solution which maximizes the entropy of the observed brightness distribution. The essential condition that the distribution is positive definite is imposed implicitly in the MEM.

3. MEM for closure data

The true brightness distribution $B_{true}(x, y)$ in the sky and the observed brightness distribution $B(x, y)$ are related to the complex spatial visibility function $\rho(= |\rho_{mn}| \exp(i\phi_{mn}))$ through a Fourier transform relationship i.e.,

$$B(x, y) = \sum_{m=-M}^{M} \sum_{n=-N}^{N} \rho_{mn} \exp\left[-i2\pi(mx + ny)\right] \tag{5}$$

or

$$\rho_{mn} = \iint B_{true}(x, y) \exp\left[i2\pi(mx + ny)\right] dx\, dy \tag{6}$$

where x and y are the sky coordinates and m and n are the spatial coordinates; (M, N) defines the finite size of the aperture. Due to the finite size of the aperture and the discrete sampling of the uv-coverage the observed distribution, in general, will not be the same as the true distribution.

Following Nityananda and Narayan (1982) the entropy of the brightness distribution could be defined in the most general

Fig. 1. A three-element interferometer system. The arrows indicate the outputs of complex correlators

form as

$$E = \iint f[B(x, y)] \, dx \, dy \qquad (7)$$

where f can be any of the conventional functions, $\ln B$ (Burg, 1967) or $-B \ln B$ (Gull and Daniell, 1978; Gull and Skilling, 1984) or other functions like $B^{1/2}$, $B^{3/2}$ etc.

Since the brightness distribution is real the visibility function ρ is hermitian i.e. $\rho_{mn} = \rho^*_{-m-n}$ (* represents the complex conjugate). With this modification Eq. (5) can be rewritten as

$$B(x, y) = \rho_{00} + \sum_{m=1}^{m} \sum_{n=1}^{N} |\rho_{mn}| \exp[i\phi_{mn} - i2\pi(mx + ny)]$$

$$+ \sum_{m=1}^{M} \sum_{n=1}^{N} |\rho_{mn}| \exp[-i\phi_{mn} + i2\pi(mx + ny)] \qquad (8)$$

To maximize the entropy E with respect to the unknown phases, $\partial E / \partial \phi_{mn}$ should be equal to zero. Substituting Eq. (8) in (7) and differentiating with respect to the unknown ϕ_{mn} we get

$$\frac{\partial E}{\partial \phi_{mn}} = 2|\rho_{mn}||\sigma_{mn}| \sin(\alpha_{mn} - \phi_{mn}) \qquad (9)$$

where,

$$|\sigma_{mn}| \exp[i\alpha_{mn}] \equiv \iint f'[B(x, y)] \exp[-i2\pi(mx + ny)] \, dx \, dy \qquad (10)$$

and $f'(B)$ is the derivative of $f(B)$ with respect to B. It is easy to see that Eq. (9) is satisfied by any value of ϕ_{mn} given by

$$\phi_{mn} = \alpha_{mn} + K_{mn}\pi \qquad (11)$$

where $K_{mn} = 0$ or ± 1. This indicates that there could be many maxima and minima of the entropy and the phase solution which one obtains by iterative schemes may not correspond to the global or true maximum.

It can be argued (Narayan and Nityananda, 1982) that presumably most of the solutions correspond to the saddle points in the entropy and only a small fraction of solutions represent real maxima. Even with this assumption the phase problem has multiple solutions and depending upon the starting condition the solution may converge to the nearest maximum. In this case it is apparent that positivity of the brightness distribution is not enough to provide the unique solution. However, beside the positivity if we have more a priori knowledge about the distribution, the chances of guiding the solution to the proper maximum go on increasing. One of the ways to provide information about the distribution could be in the form of closure phase. The solution becomes much more restricted when along with the positive definiteness of the image the visibility phases have to satisfy the closure relations. Therefore, from the uniqueness point of view the closure phase is going to be a very important constraint.

Since Eq. (9) gives the gradient of the entropy with respect to the unknown phases through one Fourier transform, it is relatively straightforward to maximize the entropy by any of the iterative gradient techniques. Starting from the observed distribution the phases are shifted in the direction of the gradient subject to the observational constraints until the entropy is reached to the maximum. If the closure phases were not there the obvious choice would be to shift the unknown phases in the direction of the gradient defined by Eq. (9). However, in the presence of the closure relations all the phases cannot be shifted along the gradient. Let us assume that ϕ_0 is a vector of initial visibility phases.

Then from closure relation (4) the closure phase

$$\phi_c = A \cdot \phi_0 = \text{predetermined by measurements} . \qquad (12)$$

If we change the visibility phases by a small amount $\Delta\phi$ the modified phases again must satisfy the closure relation (4) giving

$$A \cdot \Delta\phi = 0 \qquad (13)$$

Since we are interested in the relative changes in the observed phases, it is not required to know the absolute closure phases. If the phases satisfy the closure relations initially, a differential form of closure relation (Eq. (13)) automatically inforces the closure conditions at every stage of iteration. In Eq. (4), ϕ_c is an observationally determined vector whose elements depend upon the brightness distribution under observation, and the interferometer loops whereas, Eq. (13) does not require any observational data and is rather a characteristic equation of an N element system. The advantage of Eq. (13) over (4) is that it can be generated only once for a given interferometer system and is independent of the brightness distribution.

Since $p < q$ i.e. number of closure equations is less than the number of measured phases, Eq. (13) represents a surface in a q-dimensional space. Any vector $\Delta\phi$ lying in this surface satisfies the closure equation. The maximization of the entropy requires that the phases should be shifted in the direction of the gradient. However, maximization of the entropy is only a desirable condition whereas, the closure relations are the essential conditions. The entropy should be maximized only as much the closure conditions allow. In other words we can shift the visibility phases along that vector which lies in the closure surface and is closest to the direction of the entropy gradient. Therefore, the problem reduces to find a vector $\Delta\phi$ on the closure surface defined by Eq. (13) which has smallest distance to the gradient vector.

For Eq. (13) there are $(q - p)$ independent variables and remaining p dependent variables. Without a loss of generality let us assume that the first $(q - p)$ variables are independent. If the direction of the entropy gradient is ϕ_g, the scalar distance between the shift vector $\Delta\phi$ and the gradient is

$$S = |\phi_g - \Delta\phi| = \left\{ \sum_{i=1}^{q} (\phi_{gi} - \Delta\phi_i)^2 \right\}^{1/2} \qquad (14)$$

To obtain the shortest distance between the two vectors the derivative of S with respect to the independent phase changes

$$\frac{\partial S}{\partial \Delta\phi_j} = 0; \qquad j = 1, 2, \ldots, (q - p) \qquad (15)$$

The $(q - p)$ equations given by Eq. (15) along with the p closure relations given by Eq. (13) form a set of simultaneous equations which can be solved uniquely to give $\Delta\phi$. The geometric representation of Eqs. (13)–(15) is shown in Fig. 2.

4. Computer simulations and results

A simple iterative gradient method is implemented for the maximization of the entropy. A suitable function f is chosen to define the entropy of the brightness distribution. Although, the choice of the entropy function is not very crucial, different functions lead to slightly different solutions and for a given brightness distribution one function may provide better reconstruction than the others. However, to describe the properties of the method let us take the well known form of entropy $\ln B$. Since the entropy
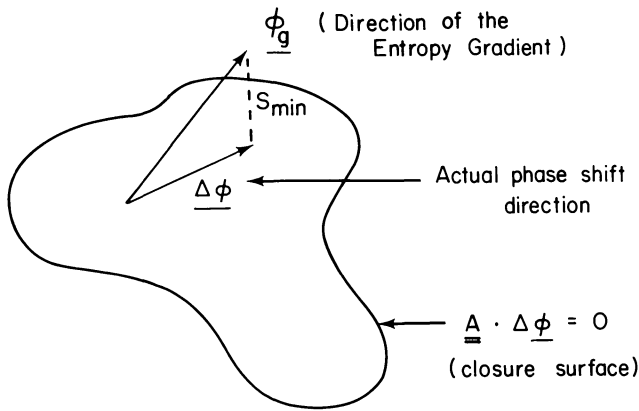
352

Fig. 2. A geometrical representation of the phase shift direction in the closure surface which is closest to the entropy gradient direction

Fig. 3. Flow diagram of the method

function is logarithmic, the brightness distribution B at every stage of iteration should be positive definite. This condition is certainly not satisfied during the initial cycles of iteration. Due to the finite size of the aperture and also due to large measurement errors the observed map contains many unwanted spurious negative and positive sources. To make the distribution positive definite during the intermediate stages of iteration, the map should be lifted by a constant background. The quality of the reconstruction does depend on the amount by which the map is lifted (Bhandari, 1978). To get a rough estimate of the constant background to be added, a parameter called the 'resolution parameter' was introduced by Nityananda and Narayan (1982) as

$$R = \frac{f''(B_{min} + C)}{f''(B_{max} + C)} \qquad (16)$$

where, $f''(B_{max} + C)$ is the second derivative of $f(B)$ with respect to B at a point where B is maximum and $f''(B_{min} + C)$ is the second derivative at a point where B is minimum, and C is the constant background added to the map.

They have shown that the parameter R essentially defines the degree of nonlinearity of the MEM reconstruction. For higher values of R (i.e. a smaller background) the reconstruction is more nonlinear giving sharper peaks in the distribution. For the phase problem R does not have much meaning as a resolution parameter. However, we see that the choice of R governs the degree of the phase refinement to some extent. For smaller values of R (i.e. a large background), practically all measured phases correspond to the maximum of the entropy and one does not get any refinement of the measured phases. On the other hand, if we choose a very high value of R (~few hundreds), instead of a refinement the measured phases may be dragged away from the true solution. It has been found by repetitive computations that usually for a value of R few tens one gets the best refinement of the phases.

A flow diagram of the algorithm is given in Fig. 3. First, a suitable entropy function is chosen in the form of f' directly (i.e. for entropy function $\ln B$, $f' = 1/B$ and so on). The observed brightness distribution is lifted by a flat background to satisfy the predetermined value of R. Taking f' of the lifted distribution the gradient of the entropy is computed by fast Fourier transform (FFT) of the f'. The square of the gradient is computed as a measure of convergence. Combining the gradient with the closure
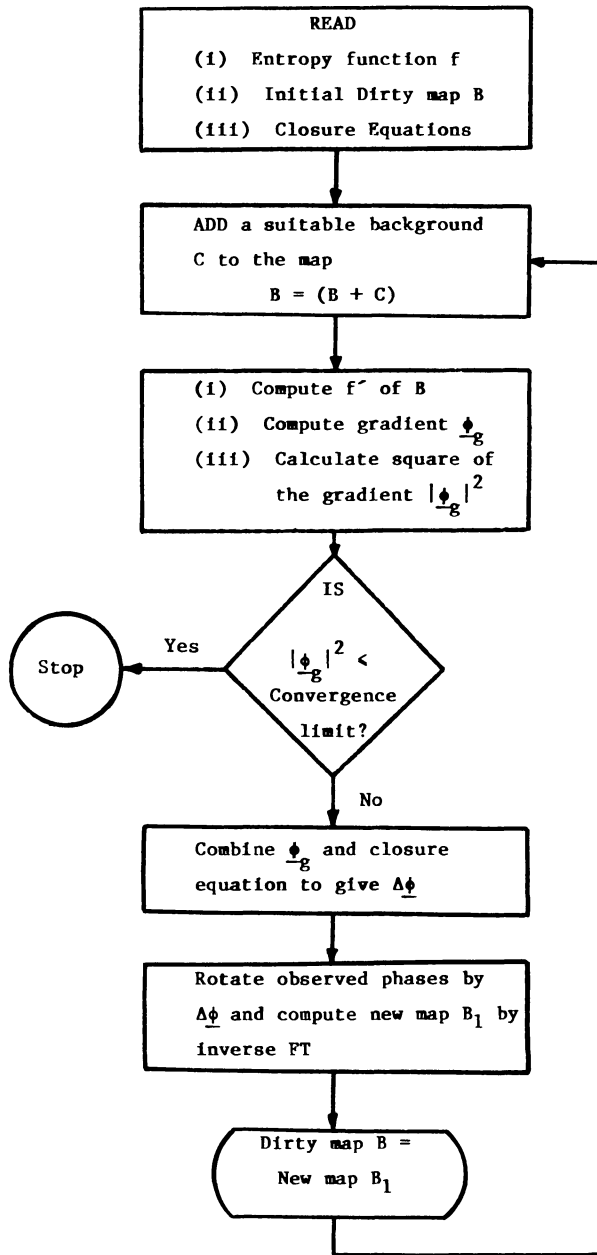
phases, the direction of the phase shift is computed. The unknown phases are rotated by the computed change in the phases. By taking an inverse Fourier transform, the new phase refined distribution is obtained. The method iterates until the square of the gradient is reached to the convergence limit. The map is lifted periodically (usually after every five iterations) to satisfy the given value of R but it is mandatory if the distribution becomes negative at any stage of iteration.

Figure 4 shows an arbitrary model brightness distribution consisting of an extended source and a localized point like source. Due to the computer limitation the total field of view in Fig. 4 is restricted to 33×33 pixels. Figure 5 shows the spatial uv-coverage plot. Since we have to write the closure relations, a direct choice of the uv-coverage is not adequate. We must define the antenna system also from which the uv-coverage is obtained.
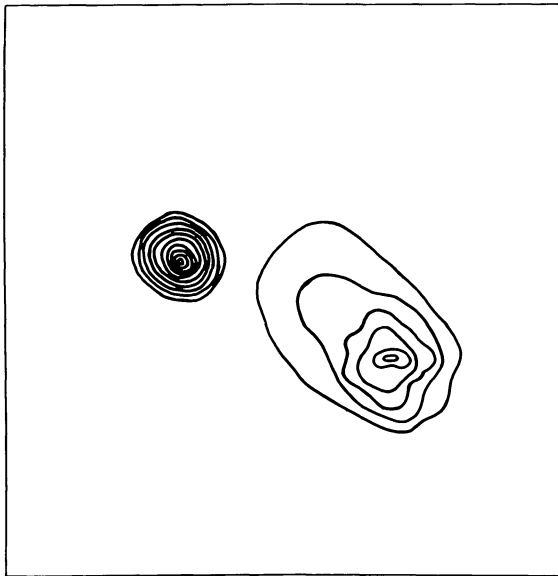
Fig. 4. A model brightness distribution map. Contour interval = 12.6 units
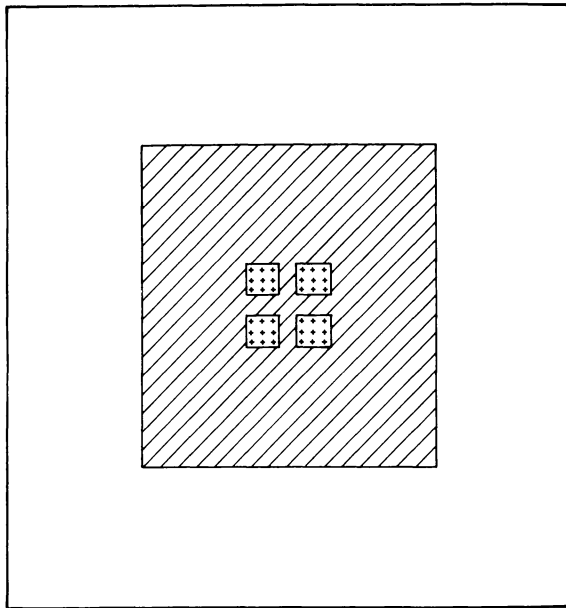

Fig. 5. A simulated uv-coverage. The region, where both amplitude and phase of the visibility function are measured, is indicated by + signs. In the hatched region the visibility amplitudes are measured accurately but the phases have large errors. In the outer empty space the visibilities are completely unknown

Let us take a synthesis telescope where all visibilities are measured simultaneously. Let us assume that there are 25 antenna elements arranged in the form of letter 'T'. The longer arm of the T is oriented along the vertical direction and the shorter arm points towards the right. If every antenna element of the system is correlated with every other element we obtain a highly redundant information which is unnecessary. Therefore, in practice the elements of the longer arm of 'T' are correlated only with the elements of the shorter arm. An antenna system of this kind, in general, provides a rectangular uv-coverage as

in Fig. 5. If all the antennas have the same order of measurement errors, all the visibilities will be affected by similar errors. However, in practice two closely spaced antennas receive radiation from the same atmospheric layers and also see the same temperature variation. Therefore, the shorter baselines generally have much less systematic errors. Just to incorporate this observational fact it is assumed that for some of the shorter spacing around the origin of the uv-plane indicated by + signs, both amplitude and phase of the visibilities are measured accurately whereas, in the hatched region the visibility amplitudes are measured more or less accurately but the phases have an rms error of ~75° (peak error ≈ ±1.5 × rms error). In the outer empty space the visibilities are completely unknown. The model map shown in Fig. 4 is Fourier transformed to have the ideal visibilities. The visibilities were forced to be zero in the outer empty space of Fig. 5. The Fourier transform of the truncated visibilities gives the map which one would have obtained from a finite uv-coverage but accurate measurement of all the visibility amplitudes and phases (Fig. 6a). Further, introducing random rms errors of ~75° in the visibility phases corresponding to the hatched area in Fig. 5, a so called observed map is obtained. This map (Fig. 6b) is the starting point of the MEM reconstruction. Assuming the above mentioned antenna configuration, the closure relations are generated by using proper visibility points. As can be seen very clearly, the observed map in Fig. 6b, apart from the real sources, shows many spurious positive and negative features. One of the strong spurious sources present in the upper left corner, has even a higher brightness than one of the true sources. Using the MEM formulation described above and taking a value of $R = 50$, the MEM map after phase refinement is shown in Fig. 7a. The MEM map shows a dramatic improvement over the observed map and is very close to the error free map in shape and intensity. If we see in terms of rms error, the initial phase error of ~75° is reduced to ~8° in 40 iterations. In fact the major refinement takes place in the first few cycles of iterations but there is recognizable refinement till ~30–40 iterations. Although, the value of R is taken to be 50, the refinement is not very sensitive to the value of R unless it is too high or too low.

In radio astronomy, so far the MEM has been used as a resolution improvement technique. In the process of resolution improvement it is usually assumed that the measured visibilities are free from all the systematic measurement errors. The observations could be affected by system noise but the noise is small compared to the measured signal (i.e., signal-to-noise ratio of each visibility is above 5σ). However, in practice these ideal conditions are met very rarely. The measured visibilities are generally affected by the measurement errors. Before computing the unknown visibilities if the measurement errors of the known visibilities are not removed, there is a high probability that the MEM image reconstruction may end up in a wrong distribution. This is demonstrated by an example here. Using the erroneous visibilities corresponding to the map in Fig. 6b, the visibilities are extrapolated in the empty region of the uv-coverage in Fig. 5. The MEM map obtained from extrapolated visibility function is shown in Fig. 8. Although the features in the map are sharpened, there is not much of an improvement over the observed map (Fig. 6b). On the other hand, if we first do the refinement of the measured visibility phases and then extrapolate the visibility function we obtain a better image reconstruction as shown in Fig. 7b. When the high resolution map obtained after the phase
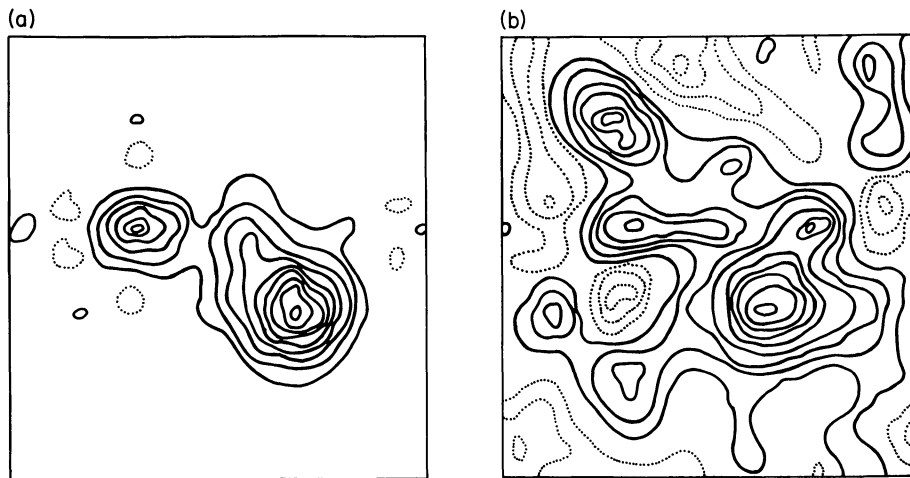
354

(a)

(b)

Fig. 6. a The error free map which one would have obtained if all the measured visibilities were accurate. Contour interval = 6.6 units. **b** Observed map with an rms phase error of ~75°. Contour interval = 4.1 units
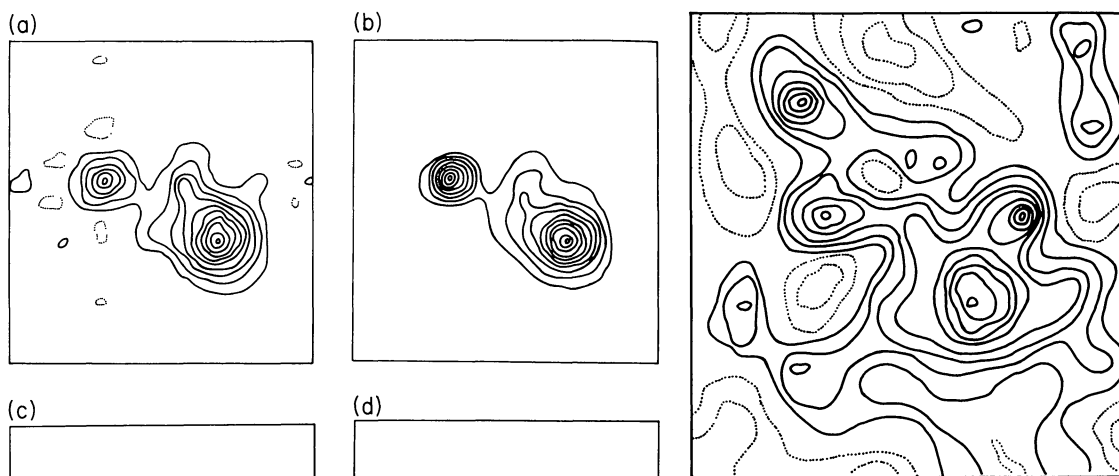
(a)

(b)

(c)

(d)

Fig. 7. a MEM phase refined map with the closure constraints. Contour interval = 6.8 units. **b** High resolution MEM map obtained from the phase refined map in **a**. Contour interval = 8.2 units. **c** MEM phase refined map without the use of the closure constraints. Contour interval = 7.4 units. **d** High resolution MEM map obtained from the phase refined map in **c**. Contour interval = 9.3 units

Fig. 8. High resolution MEM map without the refinement of the measured visibility phases. Contour interval = 4.3 units

Since MEM obtains the brightness distribution which has maximum entropy subject to some observational constraints, obviously with increasing constraints i.e., more a priori information about the distribution, one expects a reconstruction closer to the true distribution. Especially in the phase problem where there are many entropy maxima the constraints provide an additional help in guiding the solution to the proper maximum. For the comparison sake we present here the phase refined MEM map without the use of closure information in Fig. 7c. Although, the overall structure is restored the localized source in the left side of the map center is relatively attenuated. In terms of rms error also we get ~60° phase error after 40 iterations compared to the starting ~75° phase error. When we extrapolate the unknown visibility from the phase refined visibilities without the use of the closure constraints we get a reconstruction (Fig. 7d) which is significantly different from the reconstruction obtained with the closure conditions (Fig. 7b) (and also the true distribution Fig. 4).

With the increasing initial phase error the application of the closure conditions becomes rather important. For large phase errors there is a possibility that the maximization of the entropy

refinement of the measured phases (Fig. 7b) is compared with the model map (Fig. 4) it appears that although the overall structure of the distribution is restored the peak of the extended source is over sharpened. However, it should be noted that this extra enhancement of the broad peak is not due to the incomplete phase refinement but is due to the inherent peak sharpening property of the MEM when used to extrapolate the visibility function.
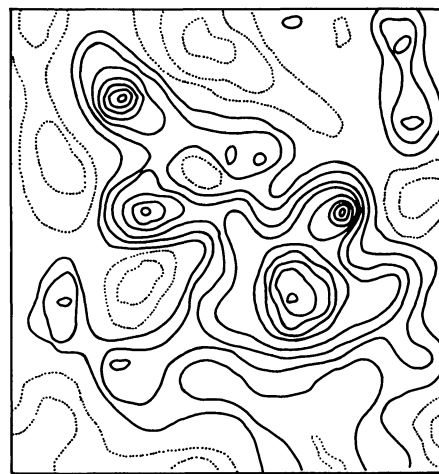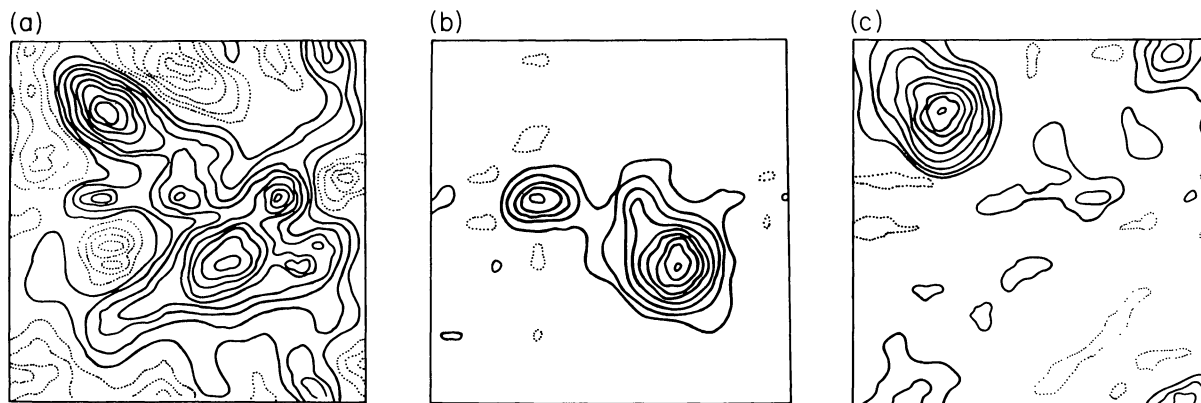
Fig. 9. a Observed dirty map with an rms visibility phase error of ∼100°. Contour interval = 3.3 units. **b** MEM phase refined map with the use of the closure constraints. Contour interval = 6.8 units. **c** MEM phase refined map without using the closure constraints. Contour interval = 6.5 units

subject to the only condition that the distribution is positive definite may give completely wrong distribution. This will become obvious from the following example.

For the same model map (Fig. 4) and same uv-coverage (Fig. 5) but relatively large rms phase error of ∼100° the observed map is shown in Fig. 9a. Starting from this map and using the same reconstruction parameters as taken above the phase refined MEM map is obtained; one with the closure constraints (Fig. 9b) and other without closure constraints (Fig. 9c). The map obtained without closure constraints does not show any resemblance to the true distribution whereas, the map with closure constraints is reconstructed reasonably well. The final rms error in the absence of the closure phases rather increases to ∼120° compared to the initial rms error of ∼100°. This is definitely an example when the MEM solution is trapped in a wrong entropy maximum. Narayan and Nityananda (1982) have expressed a hope stating that even the wrong maxima usually have some features of the true distribution. However, the above example clearly shows that in the case of a complex brightness distribution the solution corresponding to a wrong entropy maximum may not have any characteristics of the true distribution. The situation is comparatively better for a distribution composed of point-like sources. For a localised point source distribution shown in

Fig. 10a and the same initial rms phase error of 100°, although the observed dirty map shows many strong positive and negative sources (Fig. 10b), one gets reasonably good reconstruction even without the closure constraints (Fig. 10c,d). However, in Fig. 10d which is the reconstruction without closure information the sources look slightly shifted from their actual positions. If we increase the phase error further i.e. the peak phase errors are close to ±180°, although the reliability of the reconstruction reduces, the closure conditions help in obtaining the correct solution.

5. Treatment of noise in the observation

So far in our analysis, we have assumed that the noise is negligible compared to the measured visibility amplitudes over all interferometer baselines. In absence of noise although the measurements have large systematic errors, at least the closure quantities are completely error free. However, in any practical system, due to unavoidable noise, the reliability of the closure quantities themselves is in danger. Usually the system noise is independent of the choice of baseline. Since the amplitude of the visibility function is a decreasing function of baseline, for longer baselines
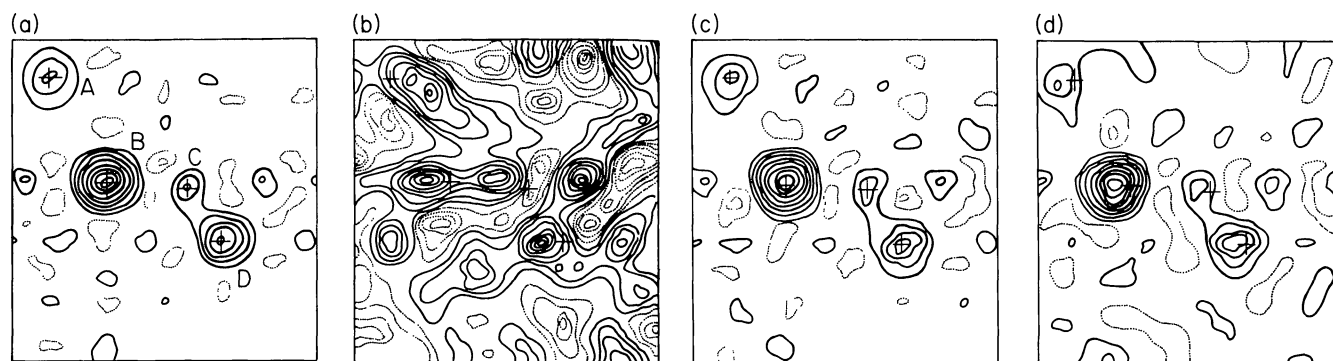

Fig. 10. a Error free brightness distribution map obtained from the finite uv-coverage (Fig. 5). The true distribution consists of four point sources A, B, C and D of intensities 50, 125, 70, and 25 units respectively. Contour interval = 4.3 units. Crosses indicate the positions of the four point sources. **b** Observed map with an rms visibility phase error of ∼100°. Contour interval = 1.9 units. **c** MEM phase refined map with the use of the closure constraints. Contour interval = 4.4 units. **d** MEM phase refined map without the use of the closure constraints. Contour interval = 4.1 units
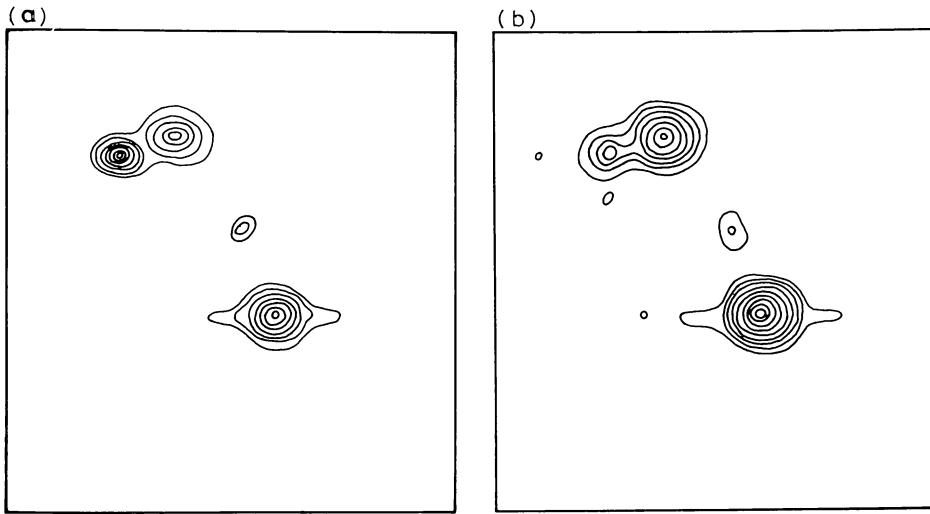
356

(a)

(b)

Fig. 11. a True image of an arbitrary distribution. Contour interval = 10.0 units. **b** Error free map obtained from a uv-coverage in Fig. 5. Contour interval = 8.6 units

the visibilities start getting dominated by the system noise. Therefore, those closure phases, which use longer interferometer baselines are more affected by the system noise.

For a noisy data, following previous authors (Ables, 1974; Willingale, 1981; Wernecke and D'Addario, 1977) the constrained entropy maximization can be converted into an unconstrained maximization of an objective function F defined as

$$F = \iint f(B)\,dx\,dy - \lambda \sum_{i=1}^{p} \frac{(\phi_{ci}^0 - \phi_{ci})^2}{\sigma_{\phi_{ci}}^2} - \mu \sum_{k=1}^{q} \frac{(\rho_k^0 - \rho_k)^2}{\sigma_{\rho_k}^2} \qquad (17)$$

where, $f(B)$ is the entropy function and λ and μ are two Lagrange multipliers. ϕ_{ci} and ϕ_{ci}^0 represent the ith estimated and measured closure phases respectively. ρ_k and ρ_k^0 are the kth estimated and measured visibility amplitudes. $\sigma_{\phi_{ci}}^2$ is the variance of the ith closure phase and $\sigma_{\rho_k}^2$ is the variance of the kth visibility amplitude. From Eq. (4), we can write

$$\phi_{ci} = \sum_{j=1}^{q} A_{ij} \phi_j \qquad (18)$$

substituting ϕ_{ci} and so ϕ_{ci}^0 from Eq. (18) into (17) we get the objective function as

$$F = \iint f(B)\,dx\,dy - \lambda \sum_{i=1}^{p} \frac{\left[\sum_{j=1}^{q} A_{ij}(\phi_j^0 - \phi_j)\right]^2}{\sum_{j=1}^{q} |A_{ij}|\sigma_{\phi_j}^2}$$

$$- \mu \sum_{k=1}^{q} \frac{(\rho_k^0 - \rho_k)^2}{\sigma_{\rho_k}^2} \qquad (19)$$

$\sigma_{\phi_j}^2$ is the variance of the phase noise for the jth visibility coefficient.

To maximize the objective function F with respect to the estimated phases and amplitudes

$$\frac{\partial F}{\partial \phi_l} = \phi_{gl} + 2\lambda \sum_{i=1}^{p} \frac{\sum_{j=1}^{q} A_{ij}(\phi_j^0 - \phi_j)}{\sum_{j=1}^{q} |A_{ij}|\sigma_{\phi_j}^2} \cdot A_{il} = 0 \qquad (20)$$

$$\frac{\partial F}{\partial \rho_k} = \rho_{gk} + 2\mu \frac{(\rho_k^0 - \rho_k)}{\sigma_{\rho_k}^2} = 0 \qquad (21)$$

ϕ_{gl} is the phase gradient corresponding to lth visibility coefficient and is given by Eq. (9). ρ_{gk} is the gradient of the entropy with respect to the kth visibility amplitude.

The Lagrange multipliers λ and μ essentially define the relative weightages given to the observational data compared to the entropy maximization. To get the best reconstruction λ and μ should be chosen by trial and error. However, we have chosen λ and μ such that the two terms in Eqs. (20) and (21) have more or less equal weightages.

The properties of the formulation are demonstrated by simulated examples. We have arbitrarily chosen a model distribution (Fig. 11) and an antenna system same as mentioned above giving a rectangular uv-coverage as shown in Fig. 5. We have restricted ourselves to the phase refinement problem without going for the estimation of unmeasured visibility coefficients. We have assumed that the visibility phases have systematic rms phase error of about 75° and on the top of that the data is corrupted by a uniformly distributed random noise. The σ of the noise is always expressed as a fraction of the integrated power of the brightness distribution, ρ_{00}.

In the first example, a noise as high as $\pm 20\%$ of ρ_{00} is assumed over all the visibilities. For an rms phase error of $\sim 75°$ the observed image is shown in Fig. 12a. The reconstructed map using $\ln B$ form of entropy is shown in Fig. 12b, after 20 iterations.

It is apparent that the reconstruction is remarkably good even for highly noisy data. One would certainly be happy with the image in Fig. 12b over the image in Fig. 12a. However, to improve the quality of the image further, the use of relative entropy function $B \ln(B/B_0)$ has been found to be very helpful (Cornwell and Evans, 1985). For defining relative entropy, using a model distribution B_0, composed of two gaussian sources located approximately at the true source positions (Fig. 13a), the reconstructed map after 20 iterations is shown in Fig. 13b. Comparison of the reconstructed images using two entropies, $\ln B$ and $B \ln(B/B_0)$ indicate that the effect of noise in the observational data can be partly compensated by biasing the reconstruction by an a priori known model distribution. Although, in this particular example the superiority of the relative entropy is not that striking, the
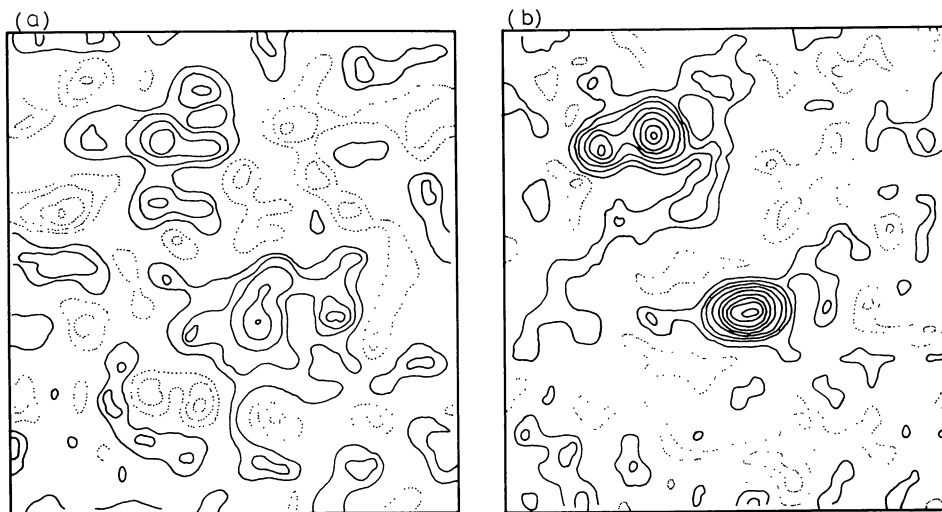
Fig. 12. a Observed map for an rms phase error of $\sim 75°$. Peak to peak measurement noise is 40% of the integrated flux of the brightness distribution. Contours are at $(-8, -6, -4, -2, 2, 4, 6, 8, 10, 12) \times 2.4$ units. **b** MEM reconstructed map after 20 iterations. Entropy function is lnB. Contour interval = 5.4 units
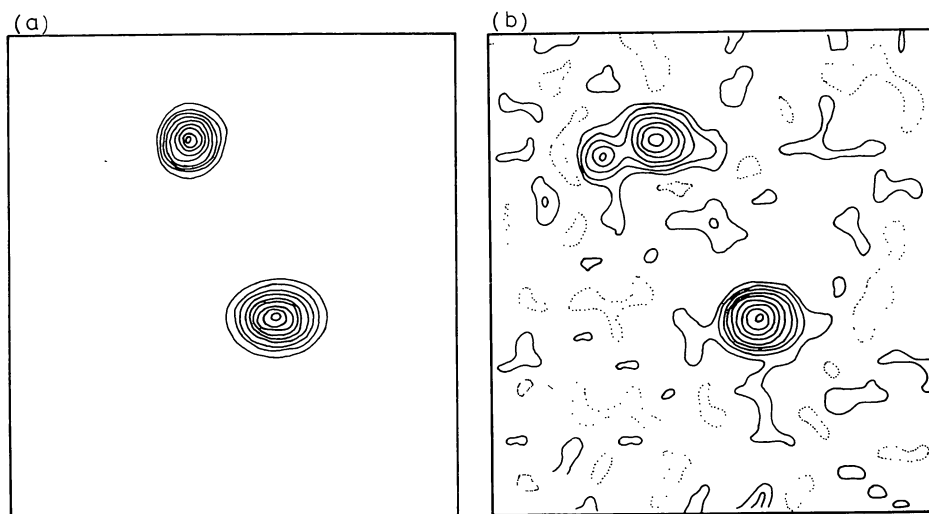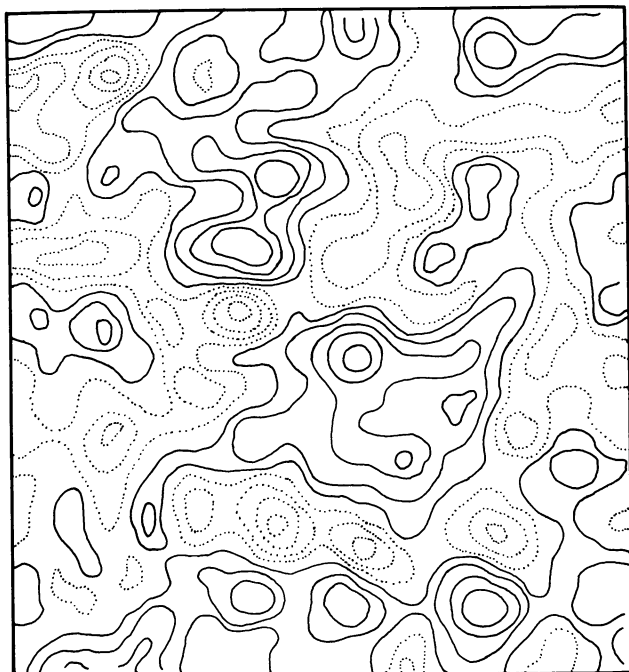

Fig. 13. a A prior model distribution B_0. Contour interval = 5.0 units. **b** Reconstructed map using relative entropy function $B \ln (B/B_0)$ after 20 iterations. Contour interval = 6.3 units

next example clearly shows that as the measurement errors increase the use of relative entropy becomes essential for noisy observations.

Let us take another example where the measurement noise is $\pm 10\%$ of ρ_{00} but the phases have an error of $\pm 120°$. The observed image (Fig. 14) in this case is so bad that retrieval of the true distribution looks almost impossible. The method has been applied to restore this distribution. Two entropy functions $\ln B$ and $B \ln (B/B_0)$ are used for the sake of comparison. For defining relative entropy function the same model with two gaussian as in Fig. 13a is used. It is clear from Fig. 15a,b that the image obtained by using relative entropy function is far superior to that obtained by simple $\ln B$ entropy. The maximization of the simple $\ln B$ entropy has not only failed in reconstructing the two upper sources, but it has also reconstructed a strong spurious source in the lower right corner of the field of view (Fig. 15a).

Fig. 14. Observed image with an rms phase error of $\sim 110°$. Peak to peak noise on the measurement is 20% of the integrated flux of the brightness distribution. Contours are at $(-9, -7, -5, -3, -1, 1, 3, 5, 7, 9, 11) \times 2.0$ units
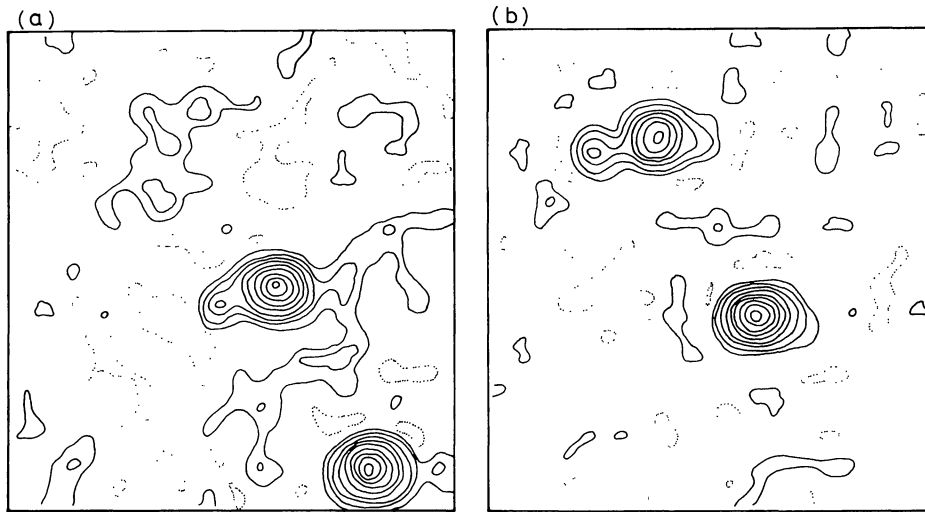
(a)   (b)

Fig. 15. a MEM reconstructed map after 20 iterations using ln B form of entropy. Contour interval = 5.0 units. **b** MEM reconstructed map after 20 iterations using relative entropy function $B \ln (B/B_0)$. Contour interval = 5.4 units

6. Concluding remarks

We have shown that the maximum entropy method which has been working reasonably well as a resolution improvement technique can be extended to improve the quality of radio astronomical images obtained from the partly phase unstable data. Before applying the MEM to the problem of resolution improvement it looks important that there should be a way to remove the observational errors from the known visibilities, as in the presence of these errors the computation of the unknown visibilities could lead to erroneous maps. The maximization of the entropy constrained with the closure phase could give remarkably good visibility phase refinement. Simple gradient method works satisfactorily to maximize the entropy by iterative technique. The method more or less converges in 30–40 iterations which in turn gives a computation time of the order of 60–80 fast Fourier transforms. Although, the closure constraints do not provide additional advantage in the phase refinement for the small phase errors and for isolated point-like sources, they are rather essential for reconstructing complex distributions and for large phase errors. In the presence of noise, when the closure phases are not accurately known, the reliability of the reconstruction can be greatly increased by biasing the reconstruction with a model distribution.

The image reconstruction method presented here for restoring the astronomical maps obtained from the phase unstable interferometers could be an alternative to the routinely used 'self-calibration' method. For large fields of view due to repetitive use of CLEAN, the self-calibration is more time consuming than the MEM with the closure phase. For extended structures as the performance of the CLEAN deteriorates, the MEM could be superior to the 'self-calibration'.

Finally we would like to point out that instead of the visibility phases one can formulate the entire problem in terms of the antenna phases. In the antenna oriented approach when all the visibility phase errors are expressed in terms of corresponding antenna phase errors, the total number of unknowns reduces appreciably but the Fourier relation between the brightness distribution and the antenna phases becomes more complex. There-fore, it appears that the antenna oriented approach reduces the number of unknowns only at the expense of computational complexity and may not provide a significant advantage over the visibility oriented approach presented here.

References

Ables, J.G.: 1974, *Astron. Astrophys. Suppl.* **15**, 383
Baldwin, J.E., Warner, P.J.: 1976, *Monthly Notices Roy. Astron. Soc.* **175**, 345
Bhandari, R.: 1978, *Astron. Astrophys.* **70**, 331
Cornwell, T.J., Wilkinson, P.N.: 1981, *Monthly Notices Roy. Astron. Soc.* **196**, 1067
Cornwell, T.J., Evans, K.F.: 1985, *Astron. Astrophys.* **143**, 77
Gull, S.F., Daniell, G.J.: 1978, *Nature* **272**, 686
Gull, S.F., Skilling, J.: 1984, Proc. IAU/URSI Symposium on 'Indirect Imaging', Ed. J.A. Roberts
Högbom, J.A.: 1974, *Astron. Astrophys. Suppl.* **15**, 417
Jennison, R.C.: 1958, *Monthly Notices Roy. Astron. Soc.* **118**, 276
Narayan, R., Nityananda, R.: 1982, *Acta Crystallogra.* **A38**, 122
Narayan, R., Nityananda, R.: 1981, *Curr. Sci.* **50**, 168
Nityananda, R., Narayan, R.: 1982, *J. Astrophys. Astron.* **3**, 419
Readhead, A.C.S., Walker, R.C., Pearson, T.J., Cohen, M.H.: 1980, *Nature* **285**, 137
Readhead, A.C.S., Wilkinson, P.N.: 1978, *Astrophys. J.* **223**, 25
Wernecke, S.J., D'Addario, L.R.: 1977, IEEE Trans. Comput., **C-26**, 351
Wilkinson, P.N., Readhead, A.C.S.: 1979, Proc. IAU symposium on 'Image Formation from Coherence Function in Astronomy', Ed. C. van Schooneveld
Willingale, R.: 1981, *Monthly Notices Roy. Astron. Soc.* **194**, 359